

DISTINCTIVE FEATURES IN NEUTRONIC PERFORMANCE OF JSNS

F. MAEKAWA, K. OIKAWA, M. HARADA, M. TESHIGAWARA, T. KAI,
Y. KASUGAI, S. MEIGO, M. OOI, M. FUTAKAWA, N. WATANABE, R. KAJIMOTO,
M. NAKAMURA

*Materials and Life Science Division, J-PARC Center, Japan Atomic Energy Agency,
2-4 Shirakata-shirane, Tokai, Ibaraki, 319-1195, Japan*

and

S. TORII, T. KAMIYAMA

*Materials and Life Science Division, J-PARC Center, High Energy Accelerator Research
Organization, 1-1 Oho, Tsukuba, Ibaraki, 305-0801 Japan*

ABSTRACT

Several unique ideas have been introduced in the moderator design of JSNS at J-PARC to bring distinctive features in its neutronic performance. Through characteristic measurements of the neutron beams, it was confirmed that the distinctive features were actually realized in the neutron beams being delivered to users. This paper describes the distinctive features and their experimental confirmation.

1. Introduction

The 1-MW pulsed spallation neutron source in the Materials and Life Science Experimental Facility (MLF) in J-PARC, JSNS, was designed to provide high quality pulsed neutron beams to users. The JSNS is equipped with three supercritical hydrogen moderators at 20 K; a coupled moderator (CM), a decoupled moderator (DM) and a poisoned decoupled moderator (PM). Figure 1 illustrates configuration and structure of the three hydrogen moderators with their features and typical pulse shapes. Several unique ideas were introduced in the moderator design to bring distinctive features in neutronic performance of JSNS.

Since production of the first pulsed neutrons at JSNS on May 30, 2008 [1], we have made an effort to characterize the neutronic performance of JSNS by measuring the neutron beams with several experimental techniques. The NOBORU instrument [2, 3] at BL10 that aimed at the DM was mainly used for this purpose while some other instruments were used when needed. Most of the distinctive features in neutronic performance of JSNS have been confirmed to be actually realized through a series of the characteristic measurements. This paper describes the distinctive features and their experimental confirmation.

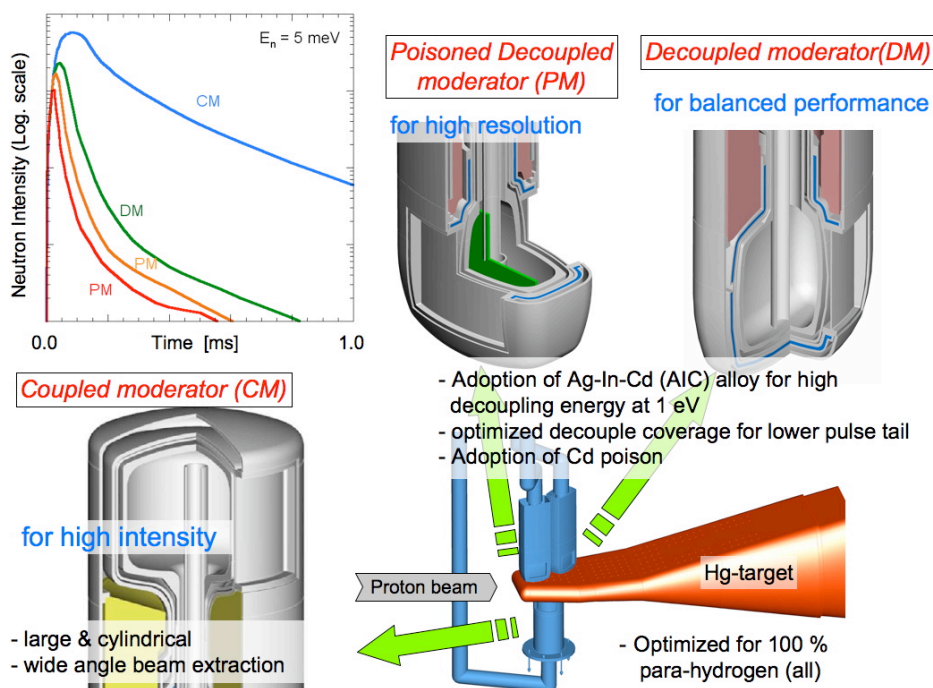


Fig. 1 Three hydrogen moderators of JSNS and typical neutron pulse shapes for the three moderators.

2. Demonstration of Distinctive Features of JSNS

2.1. Optimized for 100% Para-Hydrogen

It was found in neutronics design studies for JSNS that a hydrogen moderator with a para-hydrogen fraction of 100% was superior to those with other fractions [4-6]. Pulse peak intensity increased while pulse tail decreased as the fraction approached to 100%. Therefore, all JSNS moderators were optimized under the condition of 100% para-hydrogen. A para-hydrogen absorbs neutron energy of 14.7 meV when it transits to ortho-hydrogen by a neutron scattering. The transition process is effective to enhance cold neutron intensity. To keep the para-hydrogen fraction intentionally as close to 100% as possible, the hydrogen circulation system of JSNS is equipped with a catalyst to convert ortho-hydrogen to para-hydrogen.

Figure 2 shows the first neutron spectrum of JSNS measured by the time-of-flight (TOF) method with a Li-glass scintillator on May 2008. If neutrons achieve the thermal-equilibrium under the temperature of the cryogenic hydrogen at 20 K, the TOF spectrum should have a Maxwellian shape with a peak at 5 meV as also shown in Fig. 2. However, in reality, a sharp peak appeared at around 13 meV. The peak is a proof that the hydrogen in the moderator is para-hydrogen rich. When neutron energy goes down below several tens of meV, total cross section in para-hydrogen drops drastically by less than 1/40, having a minimum value at 13 meV as shown in Fig. 3. When a neutron above ~20 meV is scattered and its energy goes down below 20 meV, sometimes with assistance of the para-to ortho-hydrogen transition, the para-hydrogen moderator becomes very transparent suddenly due to the small cross section. When a neutron energy is above several tens of meV, the neutron stays in the moderator for a long time because a mean flight path of the neutron is about 10 mm that is rather smaller than the dimensions of the moderators. On the other hand, when a neutron energy falls down below ~20 meV, the neutron is very

likely to escape from the moderator due to the small cross section thus a longer mean flight path of ~ 200 mm. Accordingly, neutrons below ~ 20 meV can not achieve the thermal-equilibrium with the cryogenic hydrogen but make the peak at 13 meV where the cross section has a minimum value.

Figure 4 compares neutron pulse shapes measured at the JSNS's hydrogen DM and the KENS/KEK's methane DM. When the neutron energy is higher than 20 meV where the para-hydrogen cross section is still large, pulse shapes of JSNS and KENS are almost the same although the hydrogen density in the methane is 1.8 times higher than that in the para-hydrogen. When neutron energy is below 10 meV, pulse tails of the hydrogen moderator are much smaller than those of the methane moderator due to the small cross section of the para-hydrogen. Neutrons in this energy region in the methane moderator are confined in the moderator for a long time resulting in the longer pulse tails.

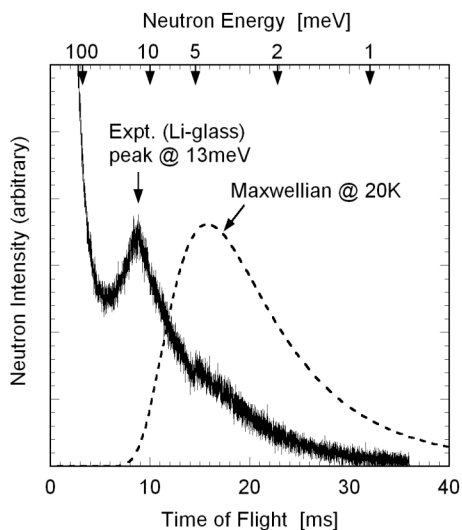


Fig. 2 The TOF spectrum for the first neutron pulse in comparison with a TOF spectrum assuming a Maxwellian distribution at 20 K.

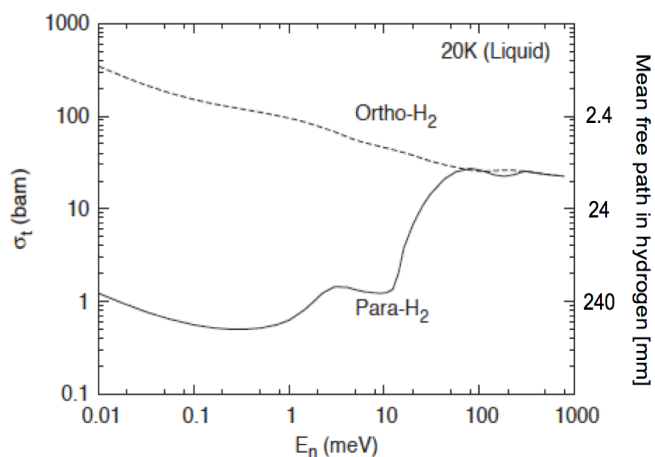


Fig. 3 Total neutron cross section in ortho- and para-hydrogen with mean-free-path of a neutron in liquid hydrogen of which weight density is 70 kg/m^3 .

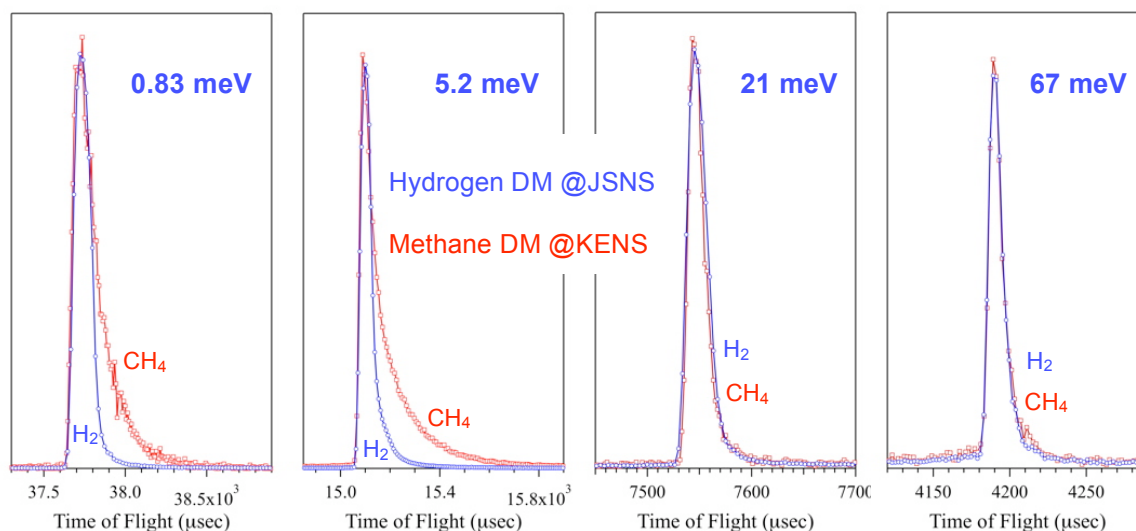


Fig. 4 Neutron pulse shapes at JSNS's hydrogen DM and KENS/KEK's methane DM in the linear scale.

ICANS XIX,
19th meeting on Collaboration of Advanced Neutron Sources
March 8 – 12, 2010
Grindelwald, Switzerland

The para-fraction close to 100% is a key parameter to achieve the high neutronic performance of JSNS. However, the 100% para-hydrogen fraction may be degraded due to radiation induced para- to ortho-hydrogen transition in the moderators when the proton beam power approaches to 1 MW. To measure the para-hydrogen fraction under the high-power operation is of importance for future development of MW-class neutron sources. We are preparing a hydrogen sampling port to take out hydrogen from the cryogenic hydrogen system to measure the para-hydrogen fraction. The Ramann spectroscopy method will be adopted to measure the para-hydrogen fraction. The relation between the proton beam power and the para-hydrogen fraction, and then the neutronic performance, will be revealed in the future.

2.2. Large Cylindrical Coupled Moderator and Its High Intensity

One of significant features in our moderator design is a unique shape of the CM. The cylindrical shape, 140 mm in diameter and 120 mm in height, is considerably larger than other existing moderators. The large dimension was born in optimization studies of the CM to maximize the neutron intensity [7, 8]. Since the cross section of the para-hydrogen in an energy range approximately below ~ 20 meV is very small, the moderator is very transparent even with the large dimension. The diameter of 140 mm was selected because neutron peak intensities in almost whole cold energy region took the maximum values with the diameter [8]. Recently, demand for CM by instrument scientists is increasing. The cylindrical shape is suitable for wide-angle neutron beam extraction to deliver many neutron beams [8]. In fact, total 11 beam lines are extracted from two viewed surfaces of the single CM without apparent intensity loss even for wide angled beam extraction ports.

The large dimension makes the neutron flux intensity higher. We have measured neutron flux intensities for almost all available neutron instruments by the gold foil activation method. The highest intensity was found at an exit of a neutron guide tube of the chopper instrument, the 4D Space Access Neutron Spectrometer (4SEASONS) [9] at beam line No. 1 aiming at the CM. A neutron flux integrated over the cutoff energy of cadmium at 0.4 eV without any choppers was 6×10^5 n/(s·cm²) at 20-kW beam power. When the beam power will be increased to 1 MW in the future, the neutron flux will be 3×10^9 n/(s·cm²) with assuming that the neutron flux is in linear relation with the proton beam power. This will be one of the most intense neutron beams that users can utilize among currently existing spallation neutron sources in the world.

2.3. Ag-In-Cd (AIC) Decoupler

A remarkable feature of the DM and PM is a rather high decoupling energy at 1 eV. This was achieved by adopting uniquely the AIC alloy [6, 10-12] as the decoupler material to make pulse widths narrower and pulse tails lower in an energy range from around 10 meV to over 1 eV. The decoupling energy of 1 eV is highly demanded by some experimenters, such as total scattering, high-resolution spectroscopy approaches to eV, and so on. Experimental results with taking advantage of the high decoupling energy will be obtained in the future.

The DM and PM are surrounded by a beryllium reflector in which thermal neutrons are alive for a long time. The decoupler prevents such thermal neutrons in the beryllium reflector from coming into the hydrogen region. Neutrons leaking into the hydrogen region with time delay deteriorate pulse shapes, especially in their pulse tails. Hence very careful consideration on which parts of the moderator should be covered with the decoupler is required to exert capability of the decoupler to the fullest. Accordingly, three-dimensional

Monte Carlo calculation was repeated many times, and the decoupler configuration shown in Fig. 5 was finally determined. The cylindrical neck part of the decoupler extended to upward and that surrounding the neutron beam extraction windows like a frame highlighted in Fig. 5 were found to be very effective to shut out thermal neutrons leaking into the hydrogen region. Of course manufacturability of the decoupler configuration was considered at the same time to realize the moderators. On the other hand, the moderator vessel needed a welding line somewhere to be fabricated in the round shape. The position was also determined by the simulation calculations with considering results of mechanical strength analysis.

One of our design targets is to decrease neutron pulse tails to 1/1,000 from their pulse peaks. To confirm the target, neutron pulse shapes from the DM were measured by the diffraction method using a c-axis oriented natural mica crystal. The crystal was mounted on the sample position of NOBORU and the cylindrical ^3He counter was set at backscattering position, $2\theta = 170$ degrees where θ denotes the Bragg angle. Figure 6 shows measured neutron pulse shapes by 006 reflection of mica with calculated ones. Diffusive tail due to incompleteness of crystal structure of the sample, probably due to a stacking fault, was observed in the raising and tail part of the Bragg peaks. Nevertheless, the pulse shape data in Fig. 6 indicates that the rapid decrease of the pulse tail to 1/1,000 is realized as expected by simulation calculations.

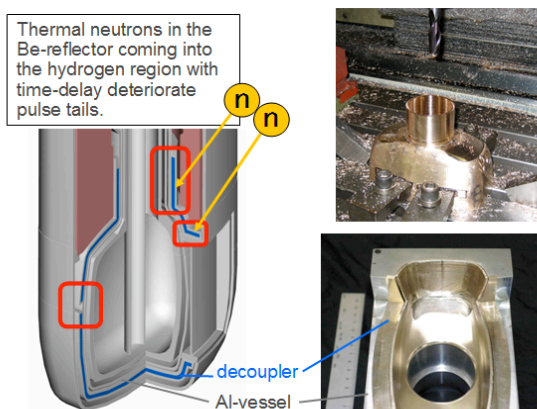


Fig. 5 Details of decoupler configuration for the DM and PM with pictures of the decoupler in fabrication..

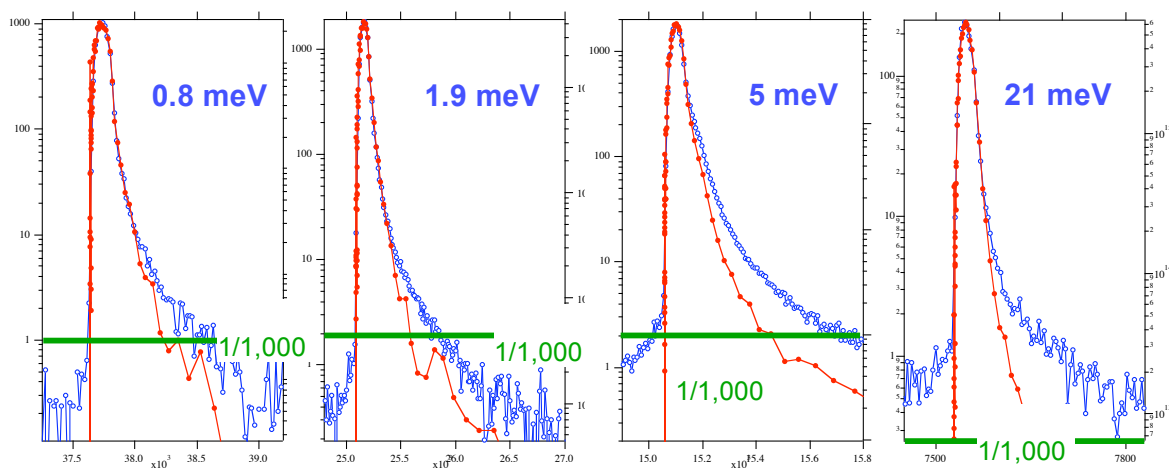


Fig. 6 Measured (symbols) and calculated (lines) pulse shapes for the DM.

2.4. High Resolution of Neutron Pulses from the Poisoned Moderator

One of the outstanding performances is the world-class resolution of the PM [1]. It is achieved with help of excellent design of an instrument, the Super High Resolution Powder Diffractometer (SuperHRPD) [13] at beam line No. 8, which have a long primary flight path of 94.2 m for better resolution. Figure 7 shows diffraction data for a single crystal silicon measured at the SuperHRPD in comparison with those measured at the Sirius instrument [14], which is a similar high-resolution powder diffractometer at KENS. No pulse tail is observed in the diffraction peak shape at SuperHRPD. The observed resolution of SuperHRPD, $\Delta d/d$, where d is a d -spacing of reflection, is 0.035%. Since the diffraction data was not corrected at a highest diffraction angle and with fine collimation of the incident beam, it is expected to be improved to the designed value 0.030% with a best experimental setup. Accordingly, the world-class resolution has been achieved at J-PARC due to excellent design of the PM and SuperHRPD.

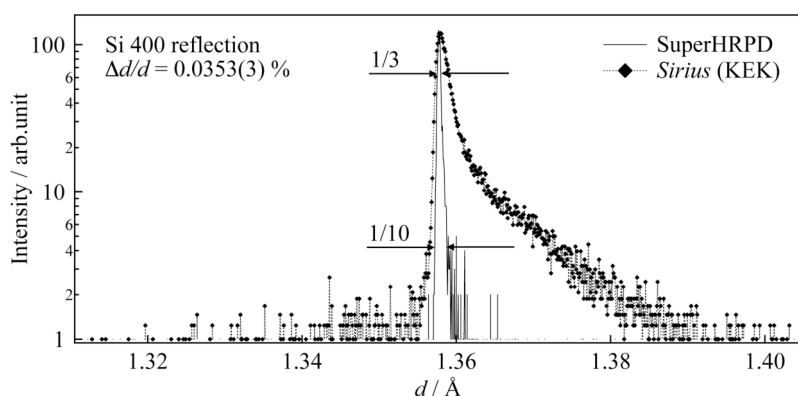


Fig. 7 Neutron diffraction data for a silicone sample measured at SuperHRPD/J-PARC and Sirius/KEK. [1]

2.5. Accurate Prediction of Neutronic Performance

A Monte Carlo particle transport simulation calculation code PHITS [15], which was an advanced version of the NMTC/JAM code [16], was extensively used for neutronic calculations of JSNS, and also for evaluating neutron beam characteristics for users. It is important to make sure that the expected neutron beams are actually delivered to users. The confirmation also gives us some hints whether the neutronic design calculations for JSNS are adequate or not. Hence we measured characteristics of neutron beams such as flux intensity, spectrum, pulse shape, etc. for available neutron instruments. The measured quantities were compared with simulation calculations.

The TOF method with calibrated ^3He and Li-glass scintillation detectors and the gold foil activation method were employed for the flux intensity measurement. With considering carefully detection efficiencies, attenuation by air and Al-windows in the beam lines, beam footprints on the detectors etc., we confirmed that the measured neutron flux intensities below 0.4 eV agreed within $\pm 20\%$ with the calculated values for all the three moderators. This good agreement was adoptable for neutron beam lines in which no guide tube was used. However, in some beam lines for which neutron guide tubes were installed, discrepancies of $1/3 \sim 1/2$ in the flux intensity were found. These discrepancies may suggest misalignment of the guide tubes, and we are investigating the reason why. Such efforts to measure neutron flux intensities at every instrument are very effective to exert the inherent ability of JSNS to the fullest.

ICANS XIX,
19th meeting on Collaboration of Advanced Neutron Sources
 March 8 – 12, 2010
 Grindelwald, Switzerland

High energy neutrons in the MeV energy region is also of interest for all instrument scientists because shield structures of all the JSNS's instruments are designed with a source term of high-energy neutrons provided by the neutron source group. Since the source term has a large impact on construction cost of the instruments, the background of the instruments and safety, the accuracy of the data needs to be studied. Application of the high-energy neutrons for study of single-upset-error of semi-conductors due to cosmic-rays is another point of interest. Accordingly, neutron flux intensity of the NOBORU instrument was measured with the foil activation method. Twelve threshold reactions shown in Fig. 8 of which sensitive energy ranged from 1 MeV to several hundreds of MeV were measured. The reaction rates were also calculated with the neutron spectrum shown in Fig. 8 and an evaluated cross section set [17]. Table 1 summarizes comparison of the measured and calculated reaction rates. Although some scatters are found in the calculated to experimental values, the calculated values agree within a factor of 2 with the experimental data. The agreement for high-energy neutrons is worse than that for cold and thermal neutron intensity, but the factor of 2 is still reasonable from a shielding point of view.

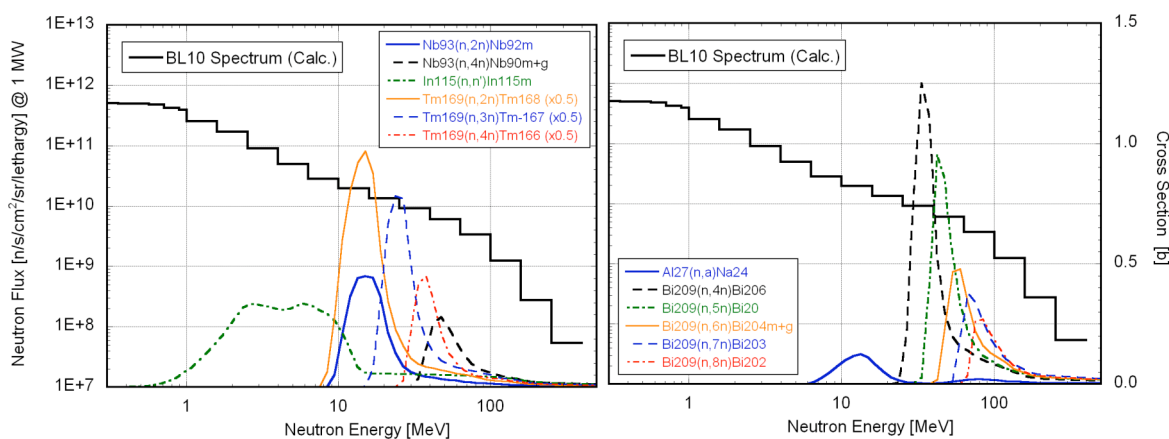


Fig. 8 High-energy neutron spectral flux at the sample position (L=14m) of the NOBORU instrument and cross section curves of threshold reactions used for the flux measurement.

Table 1 Comparison of the calculated and experimentally obtained threshold reaction rates with their approximate sensitive energy ranges.

Reaction	Approx. Sensitive Energy Range [MeV]	Calc./Expt.	Reaction	Approx. Sensitive Energy Range [MeV]	Calc./Expt.
$^{115}\text{In}(n,n)^{115\text{m}}\text{In}$	1 – 15	1.60	$^{169}\text{Tm}(n,4n)^{166}\text{Tm}$	30 – 60	1.57
$^{27}\text{Al}(n,\alpha)^{24}\text{Na}$	7 – 20	1.93	$^{209}\text{Bi}(n,4n)^{206}\text{Bi}$	25 – 50	1.81
$^{93}\text{Nb}(n,2n)^{92\text{m}}\text{Nb}$	12 – 25	2.00	$^{209}\text{Bi}(n,5n)^{205}\text{Bi}$	35 – 70	1.66
$^{93}\text{Nb}(n,4n)^{90\text{m}+\text{g}}\text{Nb}$	40 – 70	1.64	$^{209}\text{Bi}(n,6n)^{204}\text{Bi}$	45 – 90	1.69
$^{169}\text{Tm}(n,2n)^{168}\text{Tm}$	10 – 25	1.79	$^{209}\text{Bi}(n,7n)^{203}\text{Bi}$	60 – 120	1.88
$^{169}\text{Tm}(n,3n)^{167}\text{Tm}$	20 – 40	1.99	$^{209}\text{Bi}(n,8n)^{202}\text{Bi}$	75 – 150	1.39

ICANS XIX,
19th meeting on Collaboration of Advanced Neutron Sources
March 8 – 12, 2010
Grindelwald, Switzerland

3. Summary

The JSNS has several distinctive features in its design philosophy. The features bring suitable merits in neutron beams to users. Since the first neutron production in 2008, we have made much effort to measure characteristics of the pulsed neutron beams. The distinctive features of JSNS were confirmed to be actually realized in the pulsed neutron beams through the measurements.

References

1. M. Arai and F. Maekawa, *Nucl. Phys. News*, 19 (2009) 34.
2. K. Oikawa, et al., *Nucl. Instr. Meth.*, A 589 (2008) 310.
3. F. Maekawa, *Nucl. Instr. Meth.*, A 600 (2009) 335.
4. N. Watanabe, et al., *J. Neutron Res.*, 11 (2003) 13.
5. T. Kai, et al., *Nucl. Instr. Meth.*, A 523 (2004) 398.
6. M. Harada, et al., *Nucl. Instr. Meth.*, A 539 (2005) 345.
7. T. Kai, et al., *J. Nucl. Sci. Technol.*, 39, (2002) 120.
8. T. Kai, et al., *Nucl. Instr. Meth.*, A 550 (2005) 329.
9. R. Kajimoto, et al., *J. Neutron Res.*, 15 (2007) 5.
10. M. Teshigawara, et al., Development Status of Moderator-reflector System in JSNS, Proc. of ICANS-XVI, May 12-15, 2003, Düsseldorf-Neuss, Germany, 2003, pp. 601-611 (2003).
11. M. Teshigawara, et al., *J. Nucl. Mater.*, 356 (2006) 300.
12. M. Harada, et al., Deterioration of Pulse Characteristics and Burn-Up Effects with an Engineering Model in Japanese Spallation Neutron Source, ICANS-XVII, April 25-29, 2005, Santa Fe, New Mexico, US, pp. 700-709 (2006).
13. T. Kamiyama and K. Oikawa, Tow Powder Diffractometers at J-PARC, Proc. of ICANS-XVI, 12-15 May 2003, Düsseldorf-Neuss, Germany, 2003, pp. 309-314 (2003).
14. T. Kamiyama, et al., *Materials Science Forum*, 302 (2000) 321.
15. H. Iwase, et al., *J. Nucl. Sci. Technol.*, 39 (2002) 1142.
16. K. Niita, et al., *Nucl. Instr. Meth.*, B 184 (2001) 406.
17. F. Maekawa, et al., Production of a Dosimetry Cross Section Set Up to 50 MeV, Proc. 10th International Symposium on Reactor Dosimetry, September 12–17, 1999, Osaka, Japan, p. 417, American Society for Testing and Materials (2001).